

# Hydration is the Key for Gold Transport in CO<sub>2</sub>-HCl-H<sub>2</sub>O Vapor

*Yuan Mei<sup>1,2,\*</sup>, Weihua Liu<sup>1</sup>, Joël Brugger<sup>2</sup>, Art. A. Migdisov<sup>3</sup>, A.E. Williams-Jones<sup>4</sup>*

<sup>1</sup>CSIRO Mineral Resources, Research Way, Clayton, VIC 3168, Australia

<sup>2</sup>School of Earth, Atmosphere and the Environment, Monash University, 9 Rainforest Walk, Clayton, VIC 3800, Australia

<sup>3</sup>Earth and Environmental Division, Los Alamos National Laboratory, P.O. Box 1663, M.S. J535, Los Alamos, NM 87545, United States

<sup>4</sup>Department of Earth and Planetary Sciences, McGill University, 3450 University Street, Montreal, QC H3A 0E8, Canada

Corresponding authors: [yuan.mei@csiro.au](mailto:yuan.mei@csiro.au)

## Abstract

Carbon dioxide (CO<sub>2</sub>) is a major component of volcanic gases and ore-forming hydrothermal fluids. However, there is a poor understanding of the effect of CO<sub>2</sub> on the speciation of metal complexes and on ore mineral solubility. To address this deficiency, we conducted *ab initio* molecular dynamic (MD) simulations of the behavior of AuCl<sub>(aq)</sub> in the CO<sub>2</sub>-H<sub>2</sub>O system at 340 °C, 118-152 bar and 800 °C, 265-291 bar for CO<sub>2</sub> mole fractions ( $X_{\text{CO}_2}$ ) of 0.1-0.9. The MD simulations indicate that the linear [H<sub>2</sub>O-Au-Cl]<sup>0</sup> structure of gold chloride is not affected by CO<sub>2</sub> at  $X_{\text{CO}_2}$  up to 0.8 at 340 °C and up to 0.5 at 800 °C, whereas the “dry” [AuCl]<sup>0</sup> species predominates at  $X_{\text{CO}_2}$  >0.8 at 340 °C and >0.5 at 800 °C. The number of water molecules hydrating the AuCl<sub>(aq)</sub> complex decreases systematically with increasing CO<sub>2</sub> mole fraction and increasing temperature. Results of Au solubility experiments at 340 °C in CO<sub>2</sub>-H<sub>2</sub>O solutions show that the addition of CO<sub>2</sub> does not enhance Au solubility. We conclude that hydrated chloride species with linear geometry are the main means for transporting gold in CO<sub>2</sub>-H<sub>2</sub>O-HCl fluids, and that Au solubility decreases in CO<sub>2</sub>-bearing hydrothermal fluids as a result of the decrease in hydration of the Au complexes. This contrasts with the behavior of other divalent transition metals (*e.g.*, Fe, Co, Ni, and Zn). We attribute this contrasting behavior to differences in the electronic configuration of Au(I)/Cu(I)/Ag(I) and the divalent transition metal ions.

## Keywords

Molecular dynamic simulation, gold solubility, vapor transport, CO<sub>2</sub>-rich geo-fluids, hydration.

# 1 Introduction

Carbon dioxide (CO<sub>2</sub>) is one of the major components of geological fluids<sup>1</sup> and is the second most common magmatic volatile after H<sub>2</sub>O<sup>2</sup>. It is also a common component of the fluid inclusions trapped in minerals in a variety of hydrothermal ore deposits<sup>3</sup>. In the case of orogenic gold deposits, the abundance of CO<sub>2</sub>-rich fluid inclusions has given credence to the suggestion that CO<sub>2</sub> may have played a role in ore formation either by promoting metal transport<sup>4</sup> or deposition<sup>5</sup>.

Despite the prevalence of CO<sub>2</sub> in geological fluids, few studies have investigated the role of CO<sub>2</sub> in mineral solubility and metal speciation in hydrothermal systems. Adding CO<sub>2</sub> to water decreases the dielectric constant of the latter<sup>6-7</sup>, thereby enhancing ion-pairing<sup>6</sup>, decreasing the solubility of some minerals<sup>7-9</sup>, and decreasing hydration numbers around ions<sup>10-11</sup>. Based on studies of Cu solubility in HCl-H<sub>2</sub>O vapor (fluid density <0.2 g cm<sup>-3</sup>)<sup>12</sup>, which attributed steep increases in Cu solubility with increasing water activity to the increase in the hydration of the Cu(I) chloride complexes, van Hinsberg *et al.*<sup>13</sup> proposed that CO<sub>2</sub> fluxes can reduce ore mineral solubility and lead to the formation of potentially economic deposits. In contrast, Kokh *et al.*<sup>14</sup> concluded that CO<sub>2</sub> has no significant impact on the solubility of Au, Mo, Pt, and Cu but enhances the solubility of Fe, Zn and Sn at 450 °C and 600-700 bar (fluid density ~0.5 g cm<sup>-3</sup>). Kokh *et al.*<sup>15</sup> found that CO<sub>2</sub> had no effect on the partitioning of Fe/Cu/Au between brine and vapor at 350 °C and up to 100 bar in sulfide-rich systems, but enhanced Au partitioning into the vapor relative to Cu/Fe in the S-free system, probably via the formation of carbonyl vapor species. Overall, these studies show that the effect of CO<sub>2</sub> on Au behavior in high temperature CO<sub>2</sub>-rich vapor and supercritical fluids can be complex. They highlighted a need for a molecular-level understanding of the hydration of Au complexes in CO<sub>2</sub>-bearing fluids in order to help understand and predict the behavior of

Au in CO<sub>2</sub>-bearing fluids. Previous experimental and computational studies<sup>16-18</sup> have established that AuCl<sub>(aq)</sub> is the dominant Au complex in CO<sub>2</sub>-free low-density (<0.35 g/cm<sup>3</sup>) HCl-H<sub>2</sub>O solutions. Experimental studies<sup>16-17</sup> have shown that hydrated AuCl<sub>(aq)</sub> species are capable of carrying significant amounts of Au in acidic HCl-H<sub>2</sub>O vapors at 230-450 °C, and a MD study<sup>18</sup> revealed the correlation of the change of AuCl<sub>(aq)</sub> hydration with the fluid density.

This study explores the role of CO<sub>2</sub> in the speciation, hydration and solubility of Au using *ab initio* MD simulations coupled with a limited number of solubility experiments. The Au(I)-HCl-CO<sub>2</sub>-H<sub>2</sub>O system at 340-800 °C was chosen because CO<sub>2</sub>-bearing vapors are common in a variety of hydrothermal ore systems, and recent experimental and MD studies have provided us with a detailed understanding of Au(I) complexing and hydration in the CO<sub>2</sub>-free system<sup>17-18</sup>. The Au-Cl system is also well suited for this study on a theoretical level, because the stability of the AuCl<sub>(aq)</sub> species over a wide range of P,T, and hydration structure facilitates study of the effect of CO<sub>2</sub> on a single complex. Here, we used *ab initio* molecular dynamic simulations to investigate the changes brought upon by increasing CO<sub>2</sub> contents ( $X_{\text{CO}_2} = 0.1-0.9$ ) on the hydration of AuCl<sub>(aq)</sub>. In order to determine if the major trends predicted by the *ab initio* MD simulations are reproduced in real fluids, we performed a few exploratory solubility experiments at 340 °C in HCl-CO<sub>2</sub>-H<sub>2</sub>O fluid, complementing the data obtained by Hurtig and Williams-Jones<sup>17</sup> for the CO<sub>2</sub>-free system.

## 2 Methods

### 2.1 *Ab initio* molecular dynamics simulation

*Ab initio* MD simulations of AuCl<sub>(aq)</sub> in CO<sub>2</sub>-H<sub>2</sub>O mixture fluids were conducted using the Car-Parrinello molecular dynamics<sup>19</sup> (CPMD, code version 3.17.1) method. Our previous *ab initio* MD studies demonstrated the capacity of the CPMD to describe the geometry and nature of metal complexes (Cu(I)-HS-Cl<sup>20</sup>, Au(I)-Cl<sup>18</sup>, Au(I)-S<sub>3</sub><sup>21</sup>, Zn(II)-Cl-HS<sup>22-23</sup>, Pd(II)-

Cl-HS<sup>24</sup>) in aqueous solutions over a wide range of solution density and composition. The CPMD implements density functional theory (DFT) using a plane-wave basis set and pseudo-potentials to simulate the presence of the core electrons. The PBE exchange correlation-functional<sup>25</sup> was used with a cut-off gradient correction of  $5 \times 10^{-5}$ . Vanderbilt ultrasoft pseudo-potentials in the CPMD package were employed together with plane-wave cutoffs of 25 Ry (340.14 eV), a time-step of 3 a.u. (0.073 fs) and a fictitious electron mass of 400 a.u. ( $3.644 \times 10^{-28}$  kg). All MD simulations were performed in the NVT ensemble, and temperature was controlled by the Nosé thermostat for both the ions and electrons.

All the simulations were conducted within a  $30 \times 30 \times 30 \text{ \AA}^3$  cubic simulation box. Each simulation box contained 50 molecules of  $\text{H}_2\text{O} + \text{CO}_2$  with a  $\text{CO}_2$  mole fraction in the range from 0.1 to 0.9 (Table 1), one Au atom and one Cl atom. The chosen system allows us to investigate the role of  $\text{CO}_2$  in the fluid using first principle methods by a simple and tractable model, and also provides a direct comparison with available experimental data, which show that  $\text{AuCl}_{(\text{aq})}$  is the dominant species in low density, dilute Cl fluids<sup>8, 17</sup>. Molecular Dynamic simulations were conducted for 340 °C and 800 °C. The pressure of the simulation box was calculated using equations-of-state (EOS) for  $\text{CO}_2\text{-H}_2\text{O}$  mixtures at high T-P<sup>26-28</sup>. This provided a direct comparison between simulation and experiment as we conducted both in constant volume boxes and autoclaves, respectively. Periodic boundary conditions were applied during the simulations to eliminate surface effects. Gold(I) ions behave effectively as infinitely diluted as the distance between the Au atoms in periodic boxes is 30 Å, making Au-Au interaction are negligible. We also showed in our previous study<sup>18</sup> that the size of the simulation box (50 solvent molecules) is suitable: simulations of Cu(I)-Cl complexes in systems containing 55 or 110 water molecules provided hydration structures that were indistinguishable. Despite the relatively small total number of  $\text{CO}_2/\text{H}_2\text{O}$  molecules in this study, MD simulations with the box size of  $30 \times 30 \times 30 \text{ \AA}^3$  are relatively resource-intensive.

All the simulations were run for 29-32 picoseconds (400,000 ~ 450,000 MD steps), which is long enough to provide reasonable statistics for the structural properties, the hydration number and the solvent environment as demonstrated in our previous study<sup>18</sup>. More than two million CPU hours were used to conduct these simulations. The simulation systems chosen in this study provide a reasonable prediction of the structural properties and hydration within manageable CPU hours.

To compare the effect of adding CO<sub>2</sub> to H<sub>2</sub>O, five simulations were conducted for 340 °C with the same number of H<sub>2</sub>O molecules (15-45 H<sub>2</sub>O) and no CO<sub>2</sub> molecules (Table 1) in the simulation box. In each simulation, the initial coordination of the atoms was calculated using classical MD, applying the TIP4P potential for water and the MSM3 model for CO<sub>2</sub><sup>29</sup>, together with the approximated pair potentials derived from finite cluster calculations for Au–Cl and Au–O interactions<sup>18</sup>.

The radial distribution functions (RDF) of Au-O pairs and their integrals were calculated to obtain the average coordination number (hydration number) using VMD<sup>30</sup>. Based on the radial distribution function plots (Fig. 1a,b) of Au-O pairs and previous MD studies of Au-Cl and Cu-Cl in low-density fluids<sup>18</sup>, distance cut-offs of 3.0 Å and 5.0 Å were chosen to represent the first and second coordination shell, respectively.

## 2.2 Solubility experiment

In order to confirm the main trends predicted by the *ab initio* MD simulations, a limited set of experiments were conducted to determine Au solubility in HCl-CO<sub>2</sub>-H<sub>2</sub>O vapor at 340 °C. The experiments were performed in titanium autoclaves, and the experimental and analytical techniques were similar to those employed in previous experimental studies of metal solubility in water vapor<sup>16-17</sup>. The experimental procedures will only be described

briefly and readers are referred to these papers for further details. For each experiment, the titanium autoclaves were loaded with ~ 0.5 g of 0.01 mol/kg HCl solution, a gold wire and MoO<sub>2</sub>(s)/MoO<sub>3</sub>(s) (oxygen buffer) placed in separate quartz tubes, and a piece of dry ice (CO<sub>2</sub> solid). The precise amount of CO<sub>2</sub> in the cell was determined by weighing the cell before and after loading the dry ice, and is reported as a mole fraction in Table 2, together with other compositional data for the fluids. Experimental conditions were selected to ensure that the system was in the vapor state at 340 °C. The total pressure was estimated using the equation of state for H<sub>2</sub>O-CO<sub>2</sub> mixtures<sup>26</sup> from the known autoclave volume and the mass of H<sub>2</sub>O+CO<sub>2</sub>. The H<sub>2</sub>O fugacity was calculated using the fugacity coefficients from the HCh database<sup>31</sup>.

The experiments were run for 14 days to ensure that they reached equilibrium. Based on kinetic experiments at 300 °C<sup>16</sup>, equilibrium occurred in less than 10 days. The autoclaves were then quenched in a water bath before opening, and the condensates were collected and the autoclaves washed with a known amount (~ 5 ml) of aqua regia. Gold concentrations were measured by Neutron Activation Analysis (NAA) to an analytical precision of 10%; the detection limit was 0.8 ppb.

### 3 Results

#### 3.1 MD Results reveal the hydration structure of Au in CO<sub>2</sub>-rich fluids

The *ab initio* MD simulations revealed a systematic change in the hydration of AuCl<sub>(aq)</sub> as a function of CO<sub>2</sub> mole fraction. In all simulations, the CO<sub>2</sub> exists as individual molecules. There was no evidence of CO<sub>2</sub> complexing with Au to form stable Au-CO<sub>2</sub> species nor was carbonate (i.e., H<sub>2</sub>CO<sub>3</sub>/HCO<sub>3</sub><sup>-</sup>/CO<sub>3</sub><sup>2-</sup>) observed in the simulations (Fig. A1). For 340 °C, most

of the MD simulations ( $X_{\text{CO}_2} = 0.1\text{-}0.8$ ) predicted a distorted linear first-shell cluster,  $[\text{AuCl}(\text{H}_2\text{O})]^0$ , with an Au-Cl bond-length of 2.22 Å, consistent with results of previous X-ray absorption spectroscopic and theoretical studies<sup>18, 32-33</sup>. The Au-O RDF (Radial Distribution Function) plots (Fig. 1a) show that the length of the Au-O bond in the  $[\text{AuCl}(\text{H}_2\text{O})]^0$  clusters increases with increasing  $\text{CO}_2$  mole fraction from 2.12 Å at  $X_{\text{CO}_2} = 0.1$  to 2.17 Å at  $X_{\text{CO}_2} = 0.8$ . When  $X_{\text{CO}_2}$  reached 0.86, the water molecule in the  $[\text{AuCl}(\text{H}_2\text{O})]^0$  cluster dissociated and formed an anhydrous complex,  $[\text{AuCl}]^0$ .

For 800 °C, and  $X_{\text{CO}_2} = 0.1\text{-}0.5$ , the simulations yielded a linear first-shell cluster,  $[\text{AuCl}(\text{H}_2\text{O})]^0$ , with an Au-O bond-length of 2.17-2.18 Å, *i.e.*, slightly longer than at 340 °C (Fig. 1a,b). When  $X_{\text{CO}_2}$  reached 0.6, the bonding between Au and  $\text{H}_2\text{O}$  became less stable; a weak bond with a length of 2.0-2.8 Å was present, and corresponded to a first shell hydration number of 0.51 for a cutoff distance of 3.0 Å. With increasing  $X_{\text{CO}_2}$ , the proportion of the anhydrous complex,  $[\text{AuCl}]^0$  (*e.g.*, Fig. 1d) increased; this species was dominant at  $X_{\text{CO}_2} = 0.7$ , and reached a proportion of 99% at  $X_{\text{CO}_2} = 0.9$ .

The MD simulations also revealed changes in the number of water molecules in the second coordination shell as a function of  $X_{\text{CO}_2}$ . For example, at 340 °C, the small peak at a distance of 3-5 Å (Fig. 1a) corresponds to the second hydration shell of the Au-Cl clusters, and indicates the interaction between the first shell  $[\text{AuCl}(\text{H}_2\text{O})]^0$  cluster and water molecules in the solvent. The second  $\text{H}_2\text{O}$  shell (peak B in Fig. 1) is weakly bonded to the  $[\text{AuCl}(\text{H}_2\text{O})]^0$  cluster by H-bonds involving  $\text{H}_2\text{O}$  in the  $[\text{AuCl}(\text{H}_2\text{O})]^0$  cluster.

The simulations predict a decrease in first and second shell hydration with increasing  $\text{CO}_2$  mole fraction ( $X_{\text{CO}_2}$ ) at both 340 °C and 800 °C (Fig. 2); however, the 800 °C simulations yielded less hydration than at 340 °C at the same  $X_{\text{CO}_2}$ . The dry  $[\text{AuCl}]^0$  cluster became the



dominant species for  $X_{\text{CO}_2} > 0.8$  at 340 °C, and  $X_{\text{CO}_2} > 0.6$  at 800 °C, showing that dehydration is easier at higher temperature (Fig. 2a). The first and second shell hydration illustrated in Fig. 2b indicates that the hydration number decreases with increasing  $X_{\text{CO}_2}$ , producing a good linear correlation for 340 °C ( $R^2=0.90$ ) and 800 °C ( $R^2=0.88$ ). The first and second shell hydration number at 800 °C decreased significantly compared to that at 340 °C. At 340 °C,  $X_{\text{CO}_2} = 0.1$ , there were 3.7 water molecules (1 in the first shell and 2.7 in the second shell) surrounding Au (5 Å cutoff), whereas at 800 °C, this number decreased to 1.8 (1 in the first shell, 0.8 in the second shell).

We also conducted simulations with the same number of water molecules but without  $\text{CO}_2$  at 340 °C to test for differences in  $\text{AuCl}^0$  hydration. The same trend of increasing hydration with increasing number of  $\text{H}_2\text{O}$  molecules in the simulation box was found regardless of whether the simulation box contained only  $\text{H}_2\text{O}$  or a mixture of  $\text{H}_2\text{O}+\text{CO}_2$  (Fig. 3a). Such a trend was described for low-density  $\text{H}_2\text{O}$ -only fluids in our previous study<sup>18</sup>. However, the hydration numbers were slightly larger in the  $\text{CO}_2\text{-H}_2\text{O}$  mixed systems than in the  $\text{H}_2\text{O}$ -only systems for the same numbers of  $\text{H}_2\text{O}$  in the simulation box (Fig. 3b). Although the non-polar  $\text{CO}_2$  molecule plays a less active role in ion hydration than the polar  $\text{H}_2\text{O}$  molecule, the steric effects of the  $\text{CO}_2$  molecule resulted in slightly larger hydration numbers for mixed  $\text{CO}_2\text{-H}_2\text{O}$  mixed fluids at similar ‘water density’. In other words,  $\text{CO}_2$  appears to increase the clustering of waters around the  $\text{AuCl}_{(\text{aq})}$  moiety.

### 3.2 Solubility experiments

The results of Au solubility measurements in  $\text{HCl-CO}_2\text{-H}_2\text{O}$  vapor with  $\text{CO}_2$  mole fractions ranging from 0.4 to 0.84 are shown in Fig. 4. The measured solubility, expressed in terms of Au mole fractions, decreased with increasing  $\text{CO}_2$  mole fraction (Table 2). The measured Au concentrations in our experiments, however, are very close to the detection

limit of 0.8 ppb and three data points are similar within quoted uncertainties (Fig. 4). The results are also plotted as a function of water fugacity together with the Au solubility data in CO<sub>2</sub>-free HCl-H<sub>2</sub>O vapor at 340 °C reported by Hurtig and Williams-Jones<sup>17</sup>. These results show that, for similar water fugacity and pH conditions, our solubility results in CO<sub>2</sub> bearing vapor are similar to the values of CO<sub>2</sub>-free water vapor by Hurtig and Williams-Jones<sup>17</sup> (Fig. 4b), suggesting that adding CO<sub>2</sub> does not enhance Au solubility.

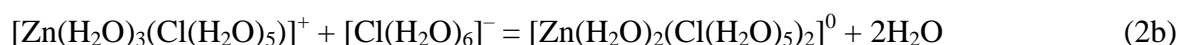
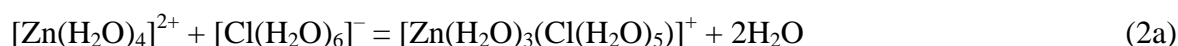
## 4 Discussion and conclusions

Our MD simulations show that H<sub>2</sub>O, a polar molecule, plays a much more active role than the non-polar CO<sub>2</sub> molecule in Au speciation in low-density H<sub>2</sub>O-CO<sub>2</sub> fluids. The CO<sub>2</sub> molecule did not bind with the Au-Cl species, and the hydration number increased with increasing mole fraction of water in the vapor. The number of H<sub>2</sub>O molecules reached a maximum of 3.7 in the first and second coordination shells of AuCl<sub>(aq)</sub> for the highest H<sub>2</sub>O/CO<sub>2</sub> ratio (10:1) at 340 °C. This is consistent with the range of hydration number (1-10) at the same temperature determined experimentally by Hurtig and Williams-Jones<sup>17</sup>. Our results also agree with those of a X-ray absorption study<sup>11</sup>, which measured a 22% decrease in the hydration number of rubidium bromide in CO<sub>2</sub>-bearing (up to 0.15 mole fraction) relative to CO<sub>2</sub>-free solutions at 445 °C. In our previous studies, we also demonstrated that hydration of Cu(I) and Au(I) chloride species is dependent on the density of water, *i.e.*, hydration decreases with decreasing fluid density<sup>18</sup>.

The new MD simulations explain the solubility behavior of Au in both the CO<sub>2</sub>-bearing vapor of this study, and previous CO<sub>2</sub>-free vapor experimental studies<sup>16-17</sup>. The simulations demonstrate that hydration is the key control of Au speciation and solubility in CO<sub>2</sub>-HCl-H<sub>2</sub>O vapor, and that CO<sub>2</sub> has a negative effect on Au solubility as Au(I)-Cl species in high T-P vapors, *e.g.*, volcanic gases, because of the dehydration of the AuCl<sub>(aq)</sub> complex. The negative

trend in solubility with increasing CO<sub>2</sub> mole fraction has been reported for the solubility of AgCl in dense H<sub>2</sub>O-CO<sub>2</sub> mixtures at 400 °C and 600-100 bar<sup>8</sup>, and for Au in H<sub>2</sub>O-CO<sub>2</sub> mixtures at 450 °C and 600-700 bar<sup>15</sup>.

Normally, the changes in hydration around Au, Cu and Ag chloride species are attributed to the decrease in the dielectric constant with increasing CO<sub>2</sub> mole fraction, following the Born equation that relates solvation energy to the dielectric constant of the solvent<sup>8</sup>. However, this simple macroscopic approach does not account for the increase in solubility of Fe, Zn and Sn minerals in CO<sub>2</sub>-bearing aqueous fluids relative to CO<sub>2</sub>-free aqueous fluids<sup>14</sup>. We propose that, at the molecular level, the change in translational entropy is the driving force behind the hydration number change as a function of CO<sub>2</sub> mole fraction in the vapor, similar to hydration behavior of Au(I) and Cu(I) complexes in low density water<sup>18</sup>, and that this explains the different solubility behavior of Au and base metals such as Zn. Consider the dehydration reaction for Au-chloride (Eq 1) and Zn-chloride complexes<sup>23</sup> (Eq 2a, b):



With an increase in the proportion of CO<sub>2</sub>, the fugacity of water decreases and therefore water is released from both the Au and Zn chloride complexes. As a result, the entropy of the system increases, driving both reactions (Eq 1 and 2) towards the right hand side. For the Au system (Eq. 1), this causes Au solubility to decrease, as shown experimentally for Au<sup>17</sup>, Ag<sup>34</sup> and Cu<sup>12</sup> in HCl-bearing vapor. In contrast, for Zn(II) (Eq. 2), this transition of the dehydration and replacement of water by chloride causes an increase in the stability constants

for the higher order chloride complexes (see data compiled for many transition metals<sup>35</sup>) and there is a corresponding increase in Zn mineral solubility.

Ultimately, the fundamental difference in the behavior of the univalent metals (*e.g.*, Au, Cu and Ag) and the divalent transition metals (*e.g.*, Zn, Fe and Ni) lies in the different electronic configurations of Au(I)/Cu(I)/Ag(I) and the first-row divalent metal ions. We attribute this contrasting behavior to the differences in coordination chemistry and affinity of chloride/bisulfide ligands for different coordination geometries. With a  $d^{10}s^1$  configuration for Cu/Ag/Au, the linear structure of Cu(I)/Ag(I)/Au(I) complexes remains unchanged and involves a maximum of two first-shell ligands (*e.g.*, the linear L-M-L complex, where M = Cu<sup>+</sup>, Ag<sup>+</sup>, Au<sup>+</sup>; L = Cl<sup>-</sup>, HS<sup>-</sup>, H<sub>2</sub>O) over a wide range of P-T conditions, salinity, and CO<sub>2</sub> contents<sup>20, 32-33, 36-38</sup>. A decrease in density or increase in CO<sub>2</sub> content will not change the geometry and the number of ligands in the first shell. In contrast, the complexes of other first-row divalent transition metal ions (*e.g.*, Zn(II)<sup>22-23, 39</sup>, Fe(II)<sup>40</sup>, Ni(II)<sup>41</sup>, Mn(II)<sup>42</sup>) undergo entropy-driven geometric changes (octahedral to tetrahedral/trigonal planar) with increasing T, decreasing pressure or density, or decreasing water activity<sup>38</sup>. Adding CO<sub>2</sub> to high-density chloride solutions will promote a decrease in coordination number, which will promote the solubility of the minerals of these first-row divalent metals (as observed by Kokh et al<sup>14</sup>). The decrease in coordination number promotes the solubility of the minerals of these first-row divalent metals because of the increased stability of the corresponding tetrahedral/trigonal planar metal-chloride complexes.

Hence, the contrast between the coordination structure of Cu(I)/Ag(I)/Au(I) and that of the divalent metals (Fe(II) and Zn(II)) helps explain why Cu/Au/Ag behave differently from other transition metals in magmatic hydrothermal fluids. In the case of Au, the subject of this paper, the linear coordination structure of the Au-Cl species ensures that hydration and thus

Au solubility will decrease with increasing  $X_{CO_2}$ . Thus the main role of CO<sub>2</sub> addition to an auriferous fluid will be to reduce Au solubility and, for porphyry-epithermal systems, the episodic fluxing of CO<sub>2</sub> from a degassing magma into the overlying hydrothermal system could be a key control of gold ore deposition, as recently demonstrated for copper<sup>13</sup>.

## Acknowledgements

Research funding was provided by the CSIRO OCE fellowship to Y.M. and by the Australian Research Council (ARC) to W.L. (FT130100510). The MD calculations in this work were supported by resources provided by the Pawsey Supercomputing Centre with funding from the Australian Government and the Government of Western Australia and the high performance computers in CSIRO. The solubility experiments were conducted in the hydrothermal laboratory at McGill University.

## References

- (1) Manning, C. E.; Shock, E. L.; Sverjensky, D. A., The Chemistry of Carbon in Aqueous Fluids at Crustal and Upper-Mantle Conditions: Experimental and Theoretical Constraints. *Rev. Mineral. Geochem.* **2013**, 75 (1), 109-148.
- (2) Lowenstern, J. B., Carbon dioxide in magmas and implications for hydrothermal systems. *Miner. Depos.* **2001**, 36 (6), 490-502.
- (3) Wilkinson, J. J., Fluid inclusions in hydrothermal ore deposits. *Litho* **2001**, 55 (1-4), 229-272.
- (4) Phillips, G. N.; Evans, K. A., Role of CO<sub>2</sub> in the formation of gold deposits. *Natur* **2004**, 429 (6994), 860-863.
- (5) Robert, F.; Kelly, W. C., Ore-forming fluids in Archean gold-bearing quartz veins at the Sigma Mine, Abitibi greenstone belt, Quebec, Canada. *Econ. Geol.* **1987**, 82 (6), 1464-1482.
- (6) Walther, J. V., Ionic association in H<sub>2</sub>O-CO<sub>2</sub> fluids at mid-crustal conditions. *Journal of Metamorphic Geology* **1992**, 10 (6), 789-797.
- (7) Walther, J. V.; Schott, J., The dielectric constant approach to speciation and ion pairing at high temperature and pressure. *Natur* **1988**, 332 (6165), 635-638.

- (8) Akinfiev, N.; Zotov, A., Thermodynamic description of equilibria in mixed fluids (H<sub>2</sub>O-non-polar gas) over a wide range of temperature (25–700°C) and pressure (1–5000 bars). *Geochim. Cosmochim. Acta* **1999**, *63* (13–14), 2025–2041.
- (9) Newton, R. C.; Manning, C. E., Hydration state and activity of aqueous silica in H<sub>2</sub>O-CO<sub>2</sub> fluids at high pressure and temperature. *Am. Mineral.* **2009**, *94* (8-9), 1287–1290.
- (10) Criscenti, L. J.; Cygan, R. T., Molecular simulations of carbon dioxide and water: cation solvation. *Environ. Sci. Technol.* **2012**, *47* (1), 87–94.
- (11) Evans, K. A.; Gordon, R. A.; Mavrogenes, J. A.; Tailby, N., The effect of CO<sub>2</sub> on the speciation of RbBr in solution at temperatures to 579 °C and pressures to 0.26 GPa. *Geochim. Cosmochim. Acta* **2009**, *73* (9), 2631–2644.
- (12) Migdisov, A. A.; Bychkov, A. Y.; Williams-Jones, A.; Van Hinsberg, V., A predictive model for the transport of copper by HCl-bearing water vapour in ore-forming magmatic-hydrothermal systems: Implications for copper porphyry ore formation. *Geochim. Cosmochim. Acta* **2014**, *129*, 33–53.
- (13) van Hinsberg, V.; Berlo, K.; Migdisov, A.; Williams-Jones, A., CO<sub>2</sub>-fluxing collapses metal mobility in magmatic vapour. *Geochem. Persp. Lett.* **2016**, *824* (LA-UR--15-28200).
- (14) Kokh, M. A.; Akinfiev, N. N.; Pokrovski, G. S.; Salvi, S.; Guillaume, D., The role of carbon dioxide in the transport and fractionation of metals by geological fluids. *Geochim. Cosmochim. Acta* **2017**, *197*, 433–466.
- (15) Kokh, M. A.; Lopez, M.; Gisquet, P.; Lanzanova, A.; Candaudap, F.; Besson, P.; Pokrovski, G. S., Combined effect of carbon dioxide and sulfur on vapor–liquid partitioning of metals in hydrothermal systems. *Geochim. Cosmochim. Acta* **2016**, *187*, 311–333.
- (16) Archibald, S. M.; Migdisov, A. A.; Williams-Jones, A. E., The stability of Au-chloride complexes in water vapor at elevated temperatures and pressures. *Geochim. Cosmochim. Acta* **2001**, *65* (23), 4413–4423.
- (17) Hurtig, N. C.; Williams-Jones, A. E., An experimental study of the transport of gold through hydration of AuCl in aqueous vapour and vapour-like fluids. *Geochim. Cosmochim. Acta* **2014**, *127*, 305–325.
- (18) Mei, Y.; Liu, W.; Sherman, D. M.; Brugger, J., Metal complexation and ion hydration in low density hydrothermal fluids: Ab initio molecular dynamics simulation of Cu(I) and Au(I) in chloride solutions (25–1000°C, 1–5000bar). *Geochim. Cosmochim. Acta* **2014**, *131* (0), 196–212.
- (19) Car, R.; Parrinello, M., Unified Approach for Molecular Dynamics and Density-Functional Theory. *Phys. Rev. Lett.* **1985**, *55* (22), 2471–2474.
- (20) Mei, Y.; Sherman, D. M.; Liu, W.; Brugger, J., Ab initio molecular dynamics simulation and free energy exploration of copper(I) complexation by chloride and bisulfide in hydrothermal fluids. *Geochim. Cosmochim. Acta* **2013**, *102* (0), 45–64.
- (21) Mei, Y.; Sherman, D. M.; Liu, W.; Brugger, J., Complexation of gold in S<sub>3</sub>-rich hydrothermal fluids: Evidence from ab-initio molecular dynamics simulations. *Chem. Geol.* **2013**, *347* (0), 34–42.
- (22) Mei, Y.; Etschmann, B.; Liu, W.; Sherman, D. M.; Testemale, D.; Brugger, J., Speciation and thermodynamic properties of zinc in sulfur-rich hydrothermal fluids: Insights from ab initio molecular dynamics simulations and X-ray absorption spectroscopy. *Geochim. Cosmochim. Acta* **2016**, *179*, 32–52.
- (23) Mei, Y.; Sherman, D. M.; Liu, W.; Etschmann, B.; Testemale, D.; Brugger, J., Zinc complexation in chloride-rich hydrothermal fluids (25–600°C): A thermodynamic model derived from ab initio molecular dynamics. *Geochim. Cosmochim. Acta* **2015**, *150* (0), 265–284.

- (24) Mei, Y.; Etschmann, B.; Liu, W.; Sherman, D. M.; Barnes, S. J.; Fiorentini, M. L.; Seward, T. M.; Testemale, D.; Brugger, J., Palladium complexation in chloride- and bisulfide-rich fluids: Insights from ab initio molecular dynamics simulations and X-ray absorption spectroscopy. *Geochim. Cosmochim. Acta* **2015**, *161* (0), 128-145.
- (25) Perdew, J. P.; Burke, K.; Ernzerhof, M., Generalized Gradient Approximation Made Simple. *Phys. Rev. Lett.* **1996**, *77* (18), 3865-3868.
- (26) Duan, Z.; Zhang, Z., Equation of state of the H<sub>2</sub>O, CO<sub>2</sub>, and H<sub>2</sub>O–CO<sub>2</sub> systems up to 10 GPa and 2573.15 K: Molecular dynamics simulations with ab initio potential surface. *Geochim. Cosmochim. Acta* **2006**, *70* (9), 2311-2324.
- (27) Hu, J.; Duan, Z.; Zhu, C.; Chou, I. M., PVTx properties of the CO<sub>2</sub>–H<sub>2</sub>O and CO<sub>2</sub>–H<sub>2</sub>O–NaCl systems below 647 K: Assessment of experimental data and thermodynamic models. *Chem. Geol.* **2007**, *238* (3–4), 249-267.
- (28) Lemmon, E.; McLinden, M.; Friend, D., Thermophysical properties of fluid systems. *NIST chemistry webbook, NIST standard reference database* **2005**, 69.
- (29) Brodholt, J.; Wood, B., Simulations of the structure and thermodynamic properties of water at high pressures and temperatures. *J. Geophys. Res. Solid Earth* **1993**, *98* (B1), 519-536.
- (30) Humphrey, W.; Dalke, A.; Schulten, K., VMD: visual molecular dynamics. *J. Mol. Graphics* **1996**, *14* (1), 33-38.
- (31) Shvarov, Y. V., HCh: New potentialities for the thermodynamic simulation of geochemical systems offered by windows. *Geochem. Int.* **2008**, *46* (8), 834-839.
- (32) Pokrovski, G. S.; Tagirov, B. R.; Schott, J.; Bazarkina, E. F.; Hazemann, J.-L.; Proux, O., An in situ X-ray absorption spectroscopy study of gold-chloride complexing in hydrothermal fluids. *Chem. Geol.* **2009**, *259* (1-2), 17-29.
- (33) Liu, W.; Etschmann, B.; Testemale, D.; Hazemann, J.-L.; Rempel, K.; Müller, H.; Brugger, J., Gold transport in hydrothermal fluids: Competition among the Cl<sup>–</sup>, Br<sup>–</sup>, HS<sup>–</sup> and NH<sub>3</sub>(aq) ligands. *Chem. Geol.* **2014**, *376* (0), 11-19.
- (34) Migdisov, A. A.; Williams-Jones, A. E., A predictive model for metal transport of silver chloride by aqueous vapor in ore-forming magmatic-hydrothermal systems. *Geochim. Cosmochim. Acta* **2013**, *104*, 123-135.
- (35) Sverjensky, D.; Shock, E.; Helgeson, H., Prediction of the thermodynamic properties of aqueous metal complexes to 1000 C and 5 kb. *Geochim. Cosmochim. Acta* **1997**, *61* (7), 1359-1412.
- (36) Brugger, J.; Etschmann, B.; Liu, W.; Testemale, D.; Hazemann, J. L.; Emerich, H.; van Beek, W.; Proux, O., An XAS study of the structure and thermodynamics of Cu(I) chloride complexes in brines up to high temperature (400°C, 600bar). *Geochim. Cosmochim. Acta* **2007**, *71* (20), 4920-4941.
- (37) Sherman, D. M., Complexation of Cu<sup>+</sup> in Hydrothermal NaCl Brines: Ab initio molecular dynamics and energetics. *Geochim. Cosmochim. Acta* **2007**, *71* (3), 714-722.
- (38) Brugger, J.; Liu, W.; Etschmann, B.; Mei, Y.; Sherman, D. M.; Testemale, D., A review of the coordination chemistry of hydrothermal systems, or do coordination changes make ore deposits? *Chem. Geol.* **2016**, *447*, 219-253.
- (39) Liu, W.; Borg, S.; Etschmann, B.; Mei, Y.; Brugger, J., An XAS study of speciation and thermodynamic properties of aqueous zinc bromide complexes at 25–150 °C. *Chem. Geol.* **2012**, *298–299* (0), 57-69.
- (40) Testemale, D.; Brugger, J.; Liu, W.; Etschmann, B.; Hazemann, J. L., In-situ X-ray absorption study of Iron (II) speciation in brines up to supercritical conditions. *Chem. Geol.* **2009**, *264* (1), 295-310.
- (41) Tian, Y.; Etschmann, B.; Liu, W.; Borg, S.; Mei, Y.; Testemale, D.; O'Neill, B.; Rae, N.; Sherman, D. M.; Ngothai, Y.; Johannessen, B.; Glover, C.; Brugger, J., Speciation of

401 nickel (II) chloride complexes in hydrothermal fluids: In situ XAS study. *Chem. Geol.* **2012**,  
402 334 (0), 345-363.  
403 (42) Tian, Y.; Etschmann, B.; Mei, Y.; Grundler, P. V.; Testemale, D.; Hazemann, J.-L.;  
404 Elliott, P.; Ngothai, Y.; Brugger, J., Speciation and thermodynamic properties of  
405 manganese(II) chloride complexes in hydrothermal fluids: In situ XAS study. *Geochim.*  
406 *Cosmochim. Acta* **2014**, 129 (0), 77-95.

407



Table 1. Simulation details for AuCl<sup>0</sup> in CO<sub>2</sub>-H<sub>2</sub>O and H<sub>2</sub>O-only fluids. Each simulation was performed in a 30 x 30 x 30 Å<sup>3</sup> cubic box.

Temperature and composition	No. of CO <sub>2</sub>	No. of H <sub>2</sub> O	X <sub>CO<sub>2</sub></sub>	fH <sub>2</sub> O (bar)	No. of AuCl <sup>0</sup>	Density (g/cm <sup>3</sup> )	Simulation time (ps)	Pressure (bar)	1 <sup>st</sup> shell* hydration	2 <sup>nd</sup> shell* hydration
340 °C  1 AuCl <sup>0</sup> , CO <sub>2</sub> +H <sub>2</sub> O	45	5	0.9	10.5	1	0.1273	31.03	152.9 <sup>a</sup>	0.04	0.20
	43	7	0.86	14.7	1	0.1241	30.88	151.9 <sup>a</sup>	0.10	0.18
	40	10	0.8	20.9	1	0.1194	31.17	150.5 <sup>a</sup>	1.00	1.09
	35	15	0.7	31.4	1	0.1114	31.17	147.6 <sup>a</sup>	1.02	2.09
	25	25	0.5	51.1	1	0.0954	29.22	140.1 <sup>a</sup>	1.01	2.80
	15	35	0.3	68.4	1	0.0794	29.79	130.5 <sup>a</sup>	1.01	3.40
	5	45	0.1	82.7	1	0.0634	29.04	118.9 <sup>a</sup>	1.04	3.73
800 °C  1 AuCl <sup>0</sup> , CO <sub>2</sub> +H <sub>2</sub> O	45	5	0.9	28.0	1	0.1273	29.58	291 <sup>c</sup>	0.01	0.07
	35	15	0.7	81.0	1	0.1114	30.15	284 <sup>c</sup>	0.18	0.49
	30	20	0.6	107	1	0.1034	29.24	281 <sup>c</sup>	0.51	0.96
	25	25	0.5	132	1	0.0954	29.55	279 <sup>c</sup>	1.01	1.50
	15	35	0.3	181	1	0.0794	30.11	271 <sup>c</sup>	1.02	1.69
	5	45	0.1	231	1	0.0634	29.41	265 <sup>c</sup>	1.02	1.75
340 °C  1 AuCl <sup>0</sup> , H <sub>2</sub> O only	0	50	0	88.3	1	0.0554	32.07	112.4 <sup>b</sup>	1.02	3.35
	0	45	0	83.9	1	0.0499	30.63	104.8 <sup>b</sup>	1.02	3.57
	0	35	0	73.2	1	0.0388	31.78	87.7 <sup>b</sup>	1.03	3.14
	0	25	0	58.6	1	0.0277	32.18	67.0 <sup>b</sup>	1.02	1.97
	0	15	0	39.4	1	0.0166	31.20	42.9 <sup>b</sup>	1.02	1.77

<sup>a,b,c</sup>Pressure was calculated from: a. the equation of state for H<sub>2</sub>O-CO<sub>2</sub> mixtures of Hu *et al.*<sup>27</sup>; b. the NIST water chemistry database<sup>28</sup>; and c. Duan and Zhang<sup>26</sup>.  
<sup>\*</sup>Distance cutoffs for the 1<sup>st</sup> and 2<sup>nd</sup> shell hydration were set at 3.0 Å and 5.0 Å, respectively<sup>18</sup>.

Table 2. Results of Au solubility experiments in CO<sub>2</sub>-HCl-H<sub>2</sub>O fluids at 340 °C. Density was estimated using the measured cell volume and total sample weight. Pressure was calculated with the equation of state for CO<sub>2</sub>-H<sub>2</sub>O mixtures<sup>26</sup>. Mole fractions (*X*) refer to the ratio of the subscripted component to the total number of moles of H<sub>2</sub>O + CO<sub>2</sub> + HCl. The H<sub>2</sub>O fugacity was calculated using the fugacity coefficients from the HCh database<sup>31</sup>.

$X_{\text{CO}_2}$	$\log f_{\text{H}_2\text{O}}$ (bar)	Density (g/cm <sup>3</sup> )	Pressure (bar)	$\log X_{\text{HCl}}$	Au (ppb)	$\log X_{\text{Au}}$
0.84	1.22	0.1358	174.0	-4.39	2.0	-9.41
0.67	1.43	0.0713	105.5	-4.11	2.9	-9.32
0.54	1.48	0.0481	79.35	-3.99	4.2	-9.20
0.44	1.46	0.0320	58.09	-3.92	12.4	-8.78

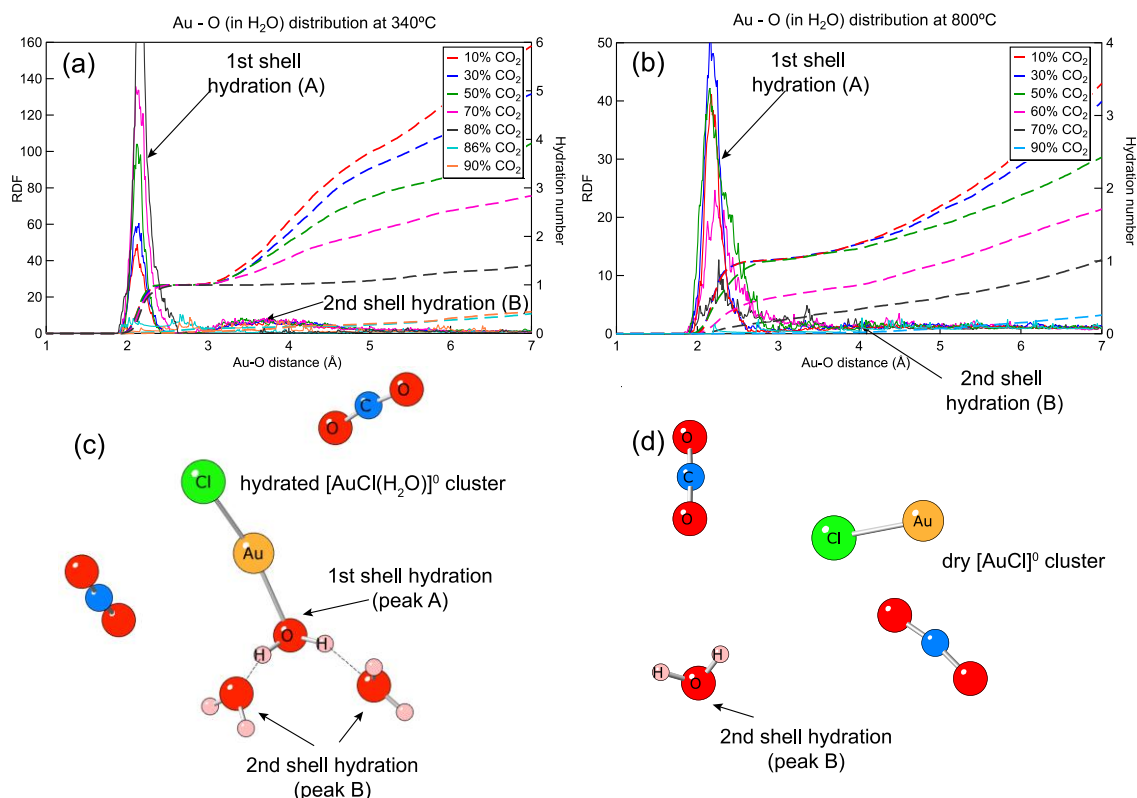


Figure 1. Radial distribution function (RDF, solid lines) and the hydration number (dash lines) of the Au-O pair at (a) 340 °C and (b) 800 °C with different  $X_{\text{CO}_2}$ ; the snapshots of MD simulations (c) at 340 °C,  $X_{\text{CO}_2} = 0.5$  and (d) at 800 °C,  $X_{\text{CO}_2} = 0.9$  show the  $\text{AuCl}_{(\text{aq})}$  and the hydration shell.

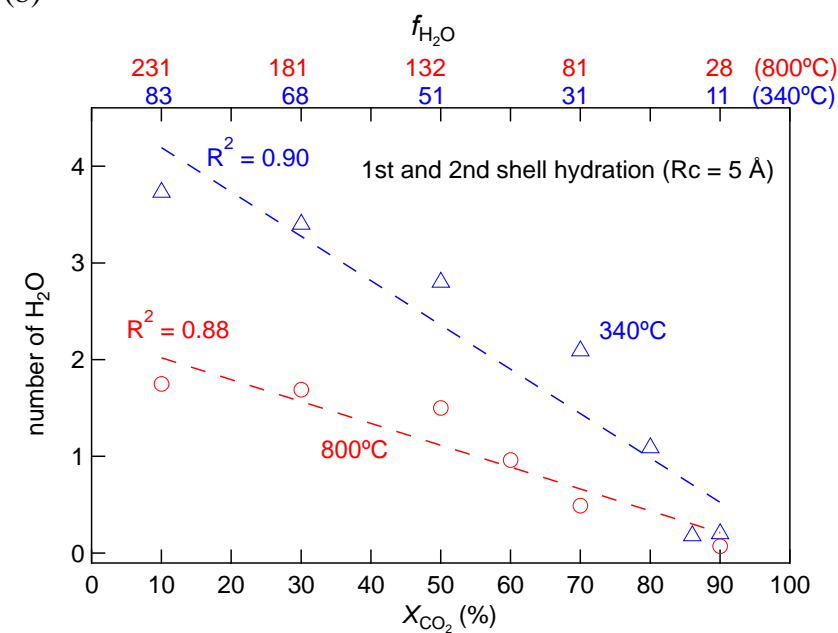
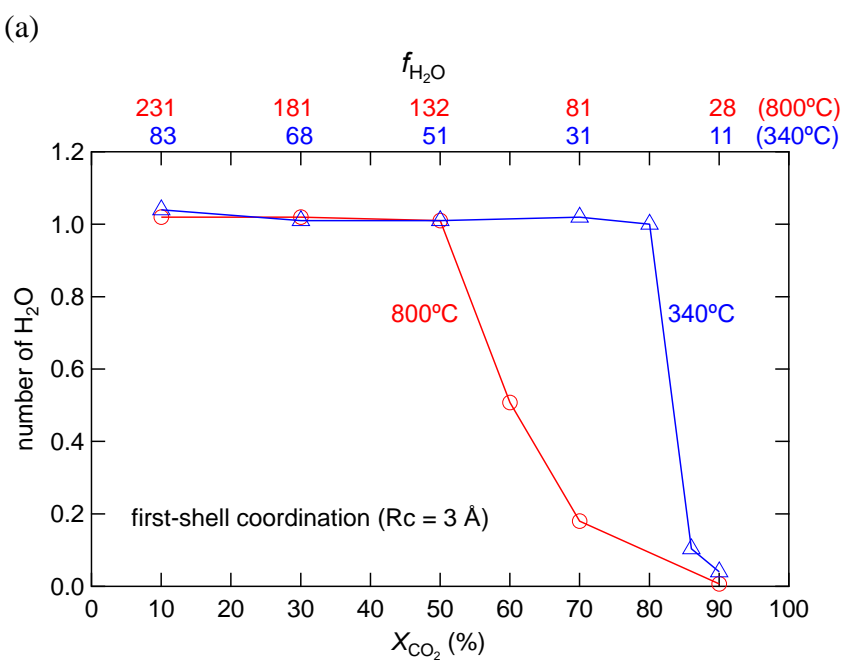


Figure 2. First shell (a) and second shell (b) hydration of Au-Cl clusters as a function of  $X_{\text{CO}_2}$  and  $X_{\text{H}_2\text{O}}$  at 340 °C (blue, triangles) and 800 °C (red, circles). The solution compositions are reported in Table 1.

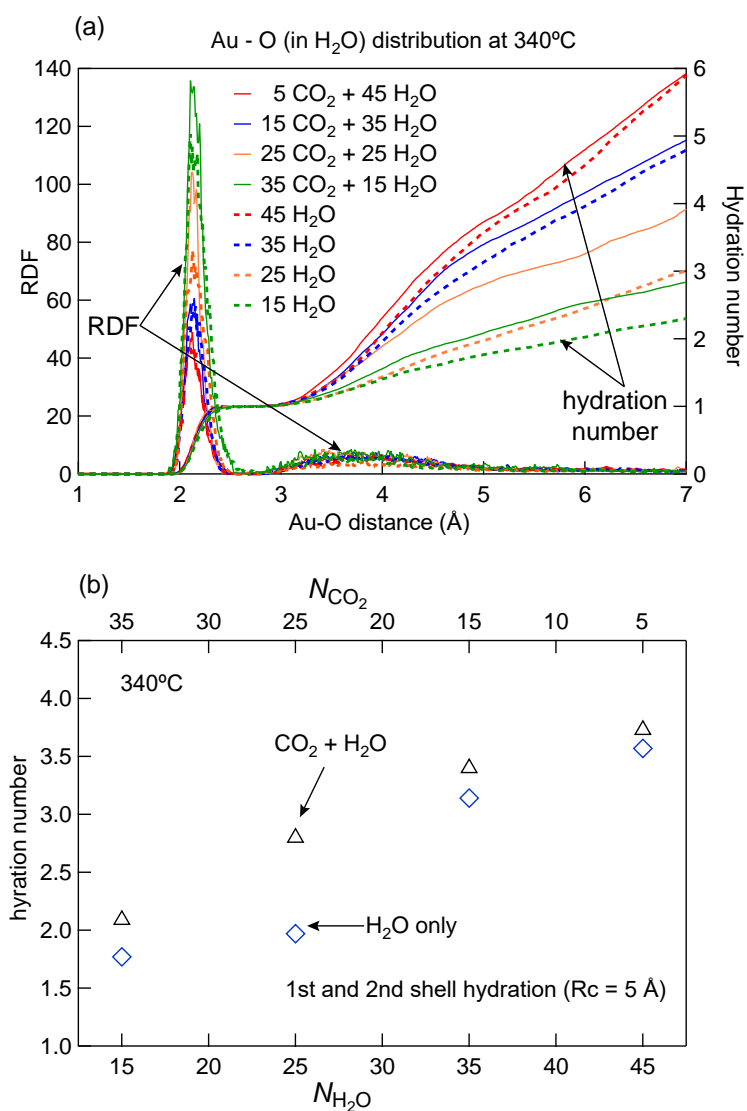


Figure 3. (a) RDF plots and (b) hydration number of AuCl<sub>(aq)</sub> for MD simulations of mixed CO<sub>2</sub>-H<sub>2</sub>O and H<sub>2</sub>O-only systems at 340 °C and a box size of 30 Å<sup>3</sup>.

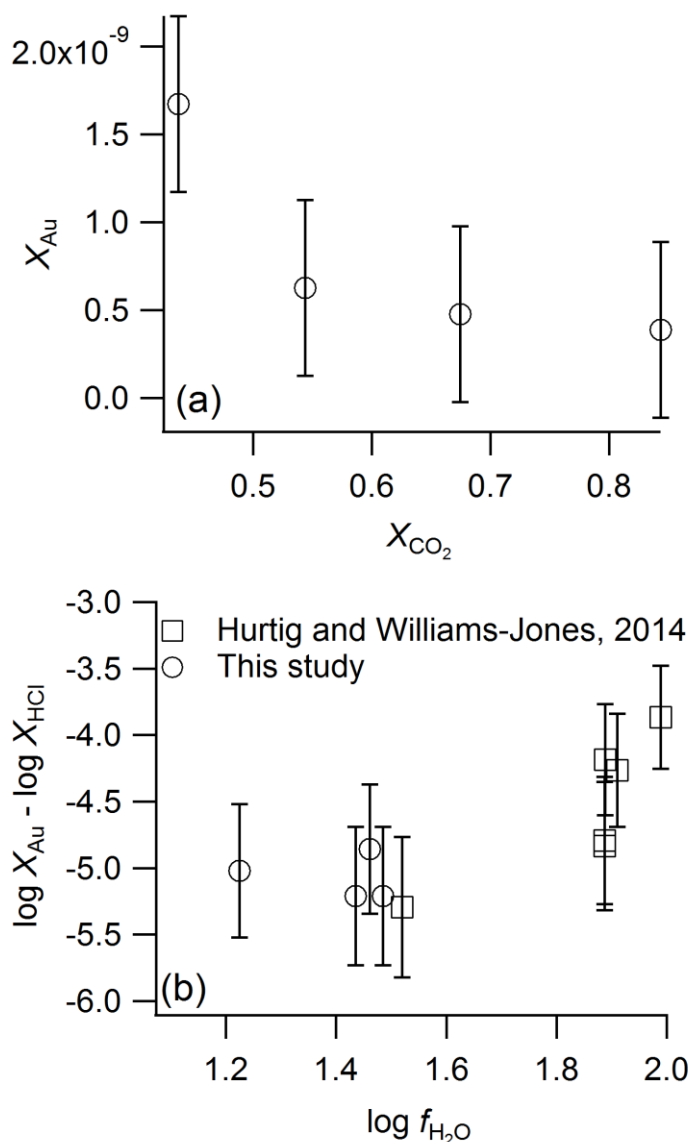
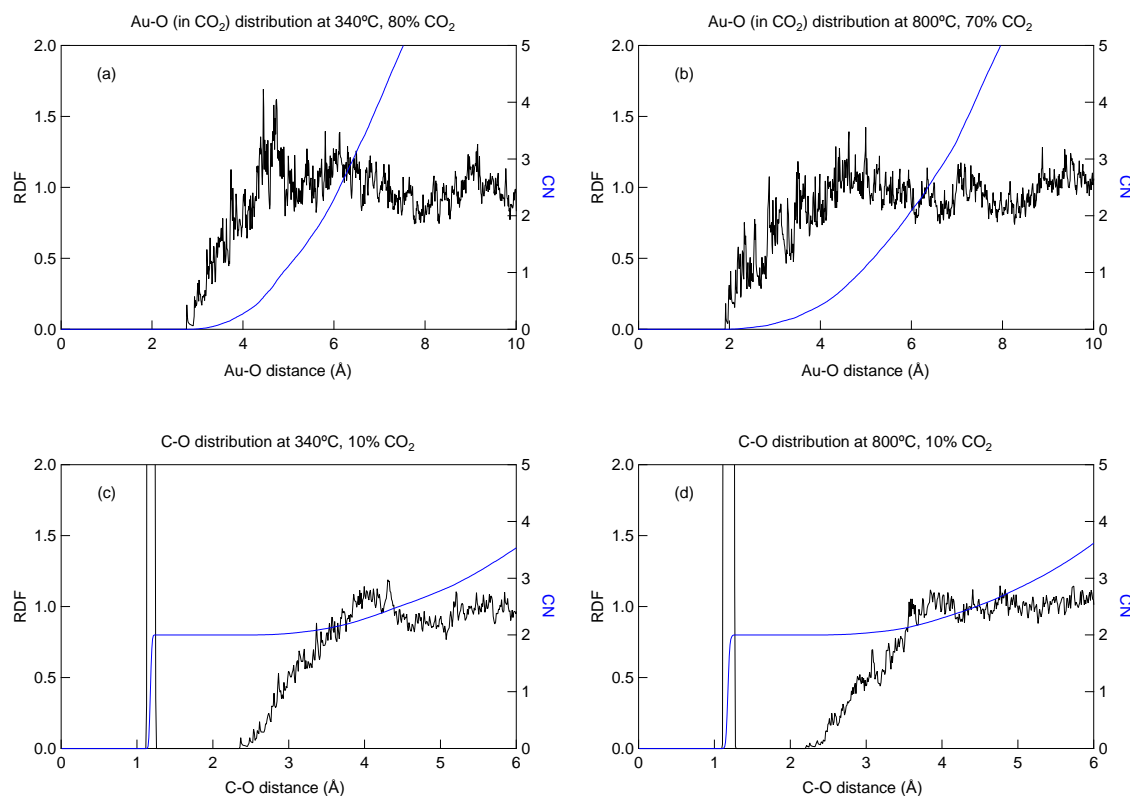


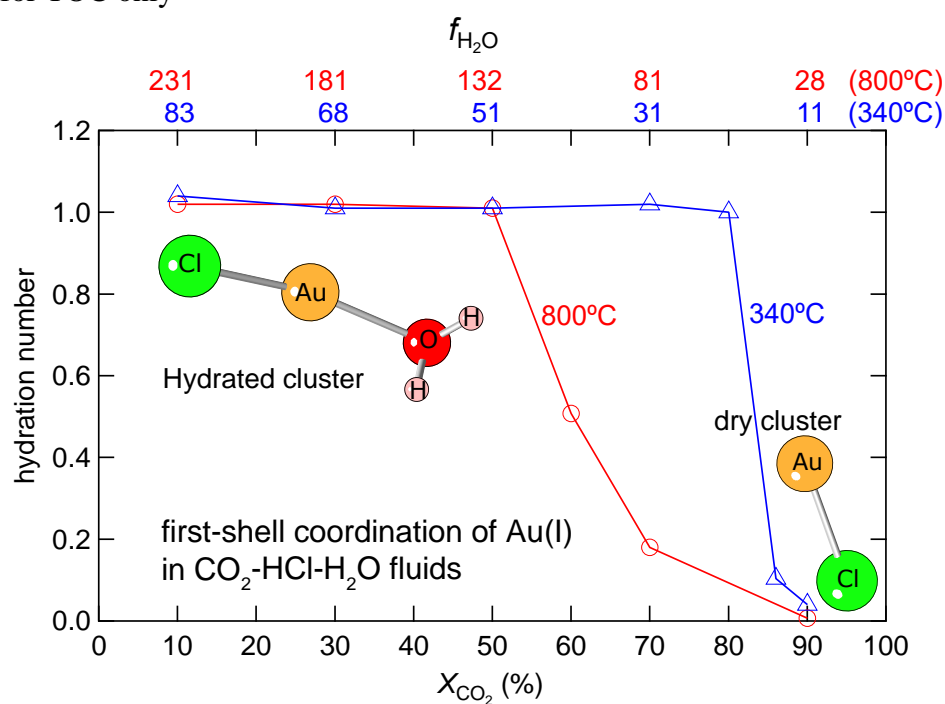
Figure 4. (a) Mole fraction of dissolved gold as a function of  $CO_2$  mole fraction in  $CO_2$ -HCl- $H_2O$  vapor at 340 °C. (See Table 1 for solution compositions). (b) Gold solubility normalized to HCl mole fraction as a function of the logarithm of water fugacity. Values of gold solubility in HCl- $H_2O$  vapor<sup>17</sup> are plotted for comparison.



445

446 Figure A1. RDF plot (black lines, left axis) and coordination number (CN, blue lines, right  
 447 axis) of (a) Au-O (O in CO<sub>2</sub>) pair at 340°C, 80% CO<sub>2</sub>; (b) Au-O (O in CO<sub>2</sub>) pair at 800°C,  
 448 70% CO<sub>2</sub>; (c) C-O pair at 340°C, 10% CO<sub>2</sub>; (d) C-O pair at 800°C, 10% CO<sub>2</sub>. Figs a,b show  
 449 that there is no bond between Au and O in CO<sub>2</sub> as there is no obvious peak between 2-3 Å.  
 450 The CN curves in Fig a,b show that within 3 Å, there are less than 0.1 oxygens from CO<sub>2</sub>  
 451 molecules surrounding Au (less than 0.05 CO<sub>2</sub> surrounding Au), indicating that there was no  
 452 complexation between Au and CO<sub>2</sub>. As shown in Figs c,d, the CN of the C-O pair within 2 Å  
 453 is two; indicating that CO<sub>2</sub> is the only carbon species, and there is no H<sub>2</sub>CO<sub>3</sub>/HCO<sub>3</sub><sup>-</sup>/CO<sub>3</sub><sup>2-</sup> in  
 454 the simulation.

455  
456 for TOC only



457